Measurement of the Mean Excitation Energy of Liquid Argon

Matthew Strait

Fermilab

19 Sept 2024

Introduction

- The mean excitation energy (*I-value*) sets energy loss of charged particles with $0.1 \lesssim \beta\gamma \lesssim 1000$:

$$\left\langle -\frac{dE}{dx} \right\rangle = Kz^2 \frac{Z}{A} \frac{1}{\beta^2} \left[\frac{1}{2} \log \frac{2m_e c^2 \beta^2 \gamma^2 W_{max}}{I^2} - \beta^2 - \frac{\delta(\beta\gamma)}{2} \right]$$

- Can't* be calculated from first principles
- Sets charged particle range, dE/dx
- First-order effect on neutrino energy reconstruction in LAr
- No near/far cancellation
- Commonly-used value (default in Geant4) 188 eV
    - From ICRU-37 (1984)
    - ICRU-90 (2016) said 187 eV

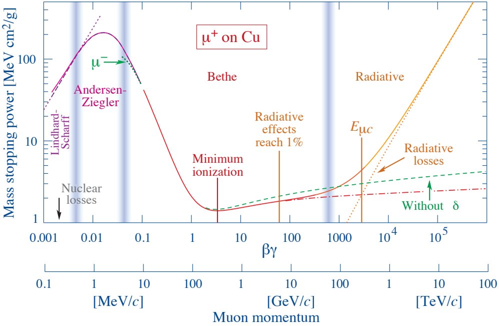

Brolley & Ribe 1955

- Let's review the five historical measurements stopping power in **gaseous** argon
- Brolley & Ribe, Phys. Rev 98 (1955) 1112
- 10.05 MeV deuterons ($\beta\gamma = 0.10$)
- Adjusted pressure in cell until energy dropped 25%
- *Stopping power* measurement (somewhat) avoiding low-energy shell corrections, etc.
- Reported $(3.72 \pm 0.08) \times 10^{-15}$ eV cm^2
- ICRU-37 (1984) inferred I-value (190 ± 15) eV
- Uncertainty: consistency between runs, i.e. "stats-only"
- CL not stated; can't assume 68% for a paper in 1955

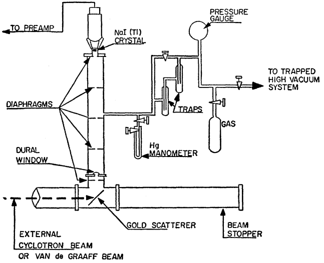

FIG. 1. Schematic diagram of apparatus for measuring stopping cross sections of gases.

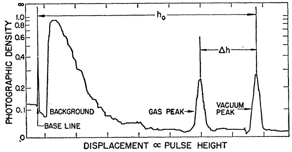

FIG. 2. Microdensitometer trace obtained by scanning the photographic negative of scintillator pulses appearing on the oscilloscope.

Martin & Northcliffe, Phys. Rev. 128 (1962) 1166.

- Stopping power of 2–10 MeV alphas ($0.03 < \beta\gamma < 0.07$) in gaseous argon
- Energy before, after measured by magnetic spectrometer
- Reported (190 ± 17) eV
- Uncertainty subjective, no particular CL: "obtained by estimating the maximum and minimum slopes consistent with the errors displayed"
- "17 eV" misread as "7 eV" by NBSIR 82-2550 (1982), propagated to ICRU-37 (1984), ICRU-90 (2016)

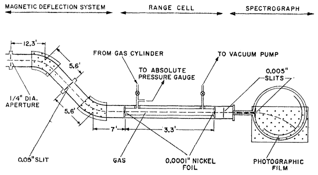

FIG. 1. Schematic plan view of the apparatus (not to scale). The path of the ions is shown by the dashed line, and the dotted areas represent regions of uniform magnetic field perpendicular to the plane of the sketch. Not shown are a pair of quadrupole focusing magnets between the aperture and the first magnet and a second pair between the second magnet and the range cell.

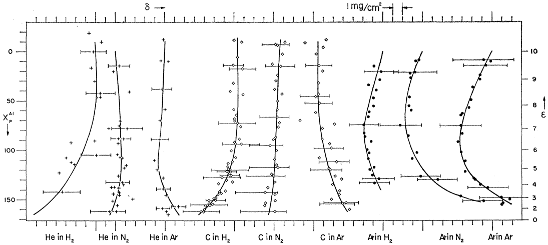

FIG. 4. Differences between the expanded curves X/β for ions in gases and the curve X_p^{Al} for protons in aluminum. The deviations from vertical are interpreted in the text in terms of the ionization potentials of the gases and the effective charges of the ions. Except for 12 points in the data for He ions in N_2 excluded because of local heating effects, all of the data for each curve are shown.

Hanke & Bichsel, K. Danske Vidensk. Selsk., Mat.-Fys. Medd. 38 (1970)

- Stopping power measurement using alphas from radioactive decay
- Reported 182 eV and 167 eV, depending on two evaluations of shell corrections
- No uncertainties stated
- ICRU-37 re-evaluated as (188 ± 10) eV, but not at all clear how this was obtained

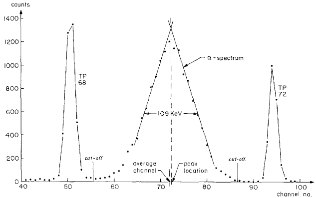

Fig. 1. Typical spectrum of alpha particles reduced in energy from $<T> = 8.782$ MeV to $<T_1> \sim 7.0$ MeV. Thus, the average energy loss is about 1.8 MeV. With the indicated cut-off points for the spectrum, the location of the mean channel is calculated to be 72.01. The "peak location" obtained by visually drawing tangent lines to the sides of the spectrum is located at 72.3 channels. The full width at half maximum obtained from the figure is 109 keV, while the calculated standard deviation for the spectrum is $\varrho = 48.4$ keV. The ratio of these two numbers is 2.26. For a gaussian, this ratio is 2.36. Two testpulses with dial readings of 68 and 72 are also shown.

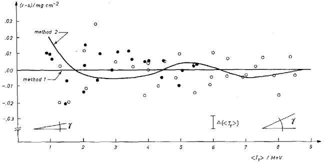

Fig. 2. Least squares fit of range difference measurements in argon. r is the calculated range difference [from eq. (7)]. The horizontal line at 0.00 mgcm^{-2} represents the fit, where the L and M-shell corrections are combined into one function, C_{L+M} (method 1). The other curve appears, when Walske's C_L is assumed to be correct, and the M-shell correction is fitted seperately (method 2). Method 1 and method 2 have rms errors 8.7 and 9.1 μgcm^{-2}, respectively. $\Delta(<T_1>)$ indicates the estimated error in (r-s) due to the total error in the energy measurements. The slope zero of the horizontal line represents the inverse of the stopping power S in Table IV, and the tangent of the angle γ indicates an 0.3 % change of S at the energies 1 and 9 MeV, respectively. ●: incident α-energy $<T> = 6.058$ MeV; ○: $<T> = 8.782$ MeV.

Besenbacher et al 1979

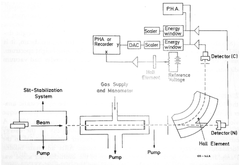

Fig. 3: Experimental setup used at the 2-MV Van de Graaff accelerator.

Fig. 10: Stopping-power results for hydrogen in argon.

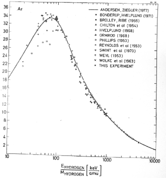

Baumgaurt et al 1983

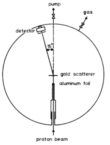

Fig. 1. Schematic view of the scattering-chamber arrangement. The diameter of the entrance aperture is 2 mm and the distance to the center 36 mm. The distance gold scatterer to detector is 221.5 mm.

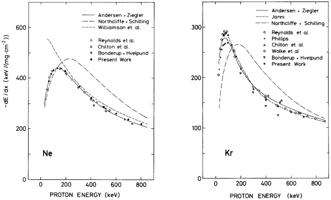

- K. Danske Vidensk. Selsk., Mat.-Fys. Medd. 40 (1979)
- Stopping power: 40 keV to 1 MeV protons, 100 keV to 2.4 MeV alphas
- Stated result: 194 eV, no uncertainties

- Nucl. Inst. Meth. 204 (1983) 597
- Stopping power: 60–800 keV protons
- Stated result: 190 eV, no uncertainties

- No clear way to derive uncertainties
- Low energy makes shell corrections a major concern

Summary of stopping power measurements

- Brolley & Ribe 1955: (190 ± 15) eV "stats"-only, maybe/probably not 68% CL
- Martin & Northcliffe 1962: (190 ± 17) eV "stats"-only, subjective
- Hanke & Bichsel 1970: 182 eV, 167 eV no uncertainties; re-evaluation: (188 ± 10) eV
- Besenbacher 1979: 194 eV no uncertainties
- Baumgart 1983: 190 eV no uncertainties

And all done at low energies where shell corrections are troublesome

- But at least there's no obvious disagreement among results

Oscillator strength distribution

- The I-value can also be determined using photoabsorption cross sections
  - Because real photon absorption is like virtual photon exchange
- Weighted sum/integral from first excitation, 11.62 eV, to ionization potential, 15.9 eV, to infinity

$$\log \mathrm{I} = \left(\sum_{\mathrm{n}} \mathrm{f_n} \log(\mathrm{E_n}) + \int_{\mathrm{IP}}^{\infty} \frac{\mathrm{df}}{\mathrm{dE}} \log(\mathrm{E}) \mathrm{dE} \right) \Big/ \mathrm{S}(0)\,,$$

$$\mathrm{S}(0) = \sum_{\mathrm{n}} \mathrm{f_n} + \int_{\mathrm{IP}}^{\infty} \frac{\mathrm{df}}{\mathrm{dE}} \mathrm{dE},$$

E: incoming photon energy
f: oscillator strength, i.e.

$$\mathrm{f} = \frac{2\epsilon_0 \mathrm{m_e c}}{\pi \mathrm{e}^2 \hbar} \sigma,$$

σ: photoabsorption cross section

Oscillator strength data

- Many sources of data for oscillator strengths, varying quality
- Use stated uncertainties if present and reliable, or estimate from paper or consistency

- Must consider data from 11.62 eV to 10 keV
- 15.9–29.3 eV contributes ±2.7 eV
  - Ok data quality; large oscillator strengths → large contributor to I-value
- 243–929 eV contributes ±2.5 eV
  - Dominated by a single group
- Just a sample. . .
- → (187 ± 5) eV

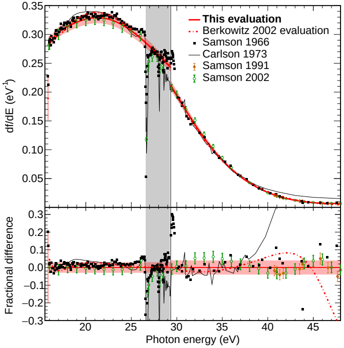

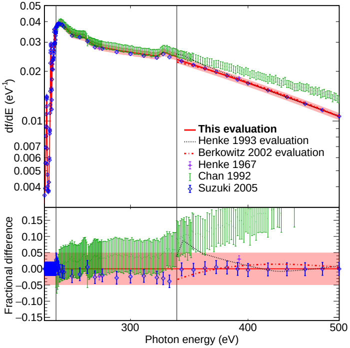

Evaluation of gaseous argon data

- Putting together stopping power measurements and OSD
- Plus a little information from periodic trends
- Plus a little information from a Hartree-Fock wave function calculation
  - Bell, Bish & Gill, J. Phys. B **5** (1972)
- $\rightarrow$ (187 ± 4) eV
  - OSD gives almost all the information!
  - Accidentally close to ICRU-90 evaluation, but many underlying differences

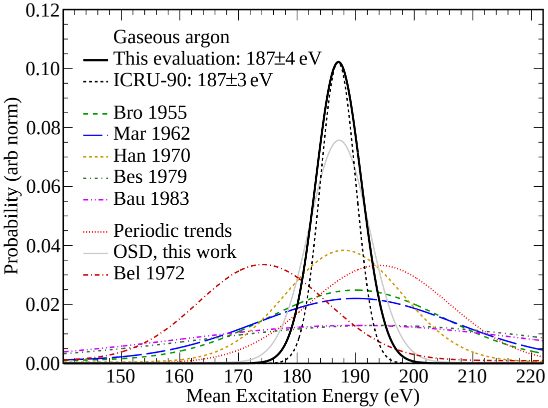

Phase effect

- Liquids are not just really dense gasses!
- Additional bonding increases I-value
- Measured as gas and liquid (ICRU-37):
    - Water
    - Hydrogen, nitrogen, oxygen
    - N-propane, pentane, hexane, heptane
- Noble gasses have lower I-values than interpolation from adjacent solid elements
- Effect decreases with Z
    - Mostly only outer electrons matter
- Trend suggests LAr is $(7 \pm 3)\%$ higher than GAr

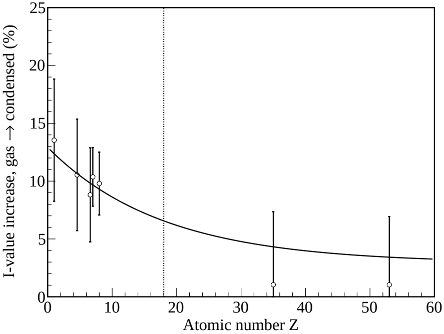

Phase effect, solid argon

- Chu et al Nucl. Inst. Meth. **149** (1978) 115: lower stopping power for 0.5–1 MeV alphas
  - But same for 1–2 MeV; Solid, gas done 7 years apart
- Besenbacher et al Nucl. Inst. Meth. **188** (1981) 657
  - $<5\%$ difference between SAr and GAr
  - Says SAr measurements are compatible with Chu

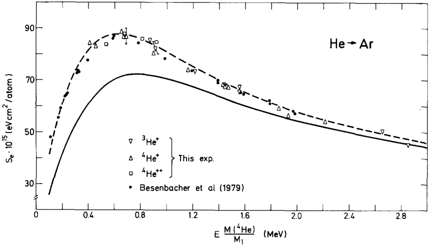

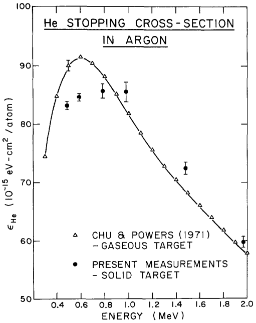

Fig. 6. Comparison of our experimental ε_{He} data in solid argon with the published gas-target data of ref. 17.

- Situation is confused, but from experiment, estimate a $(0 \pm 5)\%$ effect
- From this plus trends, estimate $(5 \pm 3)\%$ higher I-value from trends and experiment
- Best estimate for LAr: (197 ± 7) eV
  - arXiv:2212.06286; JINST 19 (2024) 01, P01009

2024 Proton Range Measurement in LAr

- 400 MeV protons from the Fermilab linac
  - Really 402.2 MeV
- LAr target contained in aluminum tub
- Measure transmission as function of beam energy
  - Energy modified via upstream copper strips

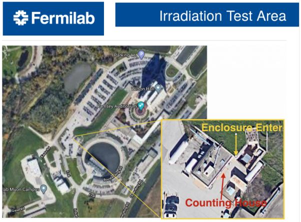

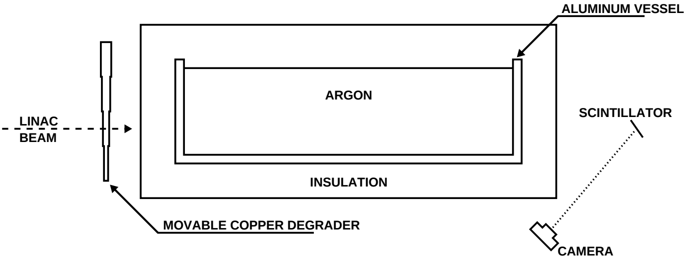


DANGER
Warning

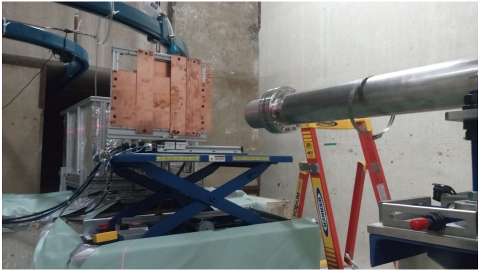

Results

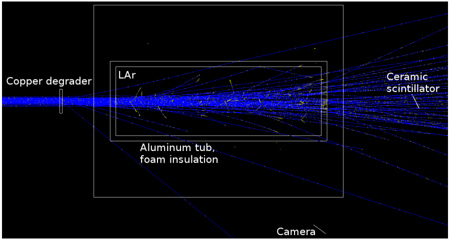

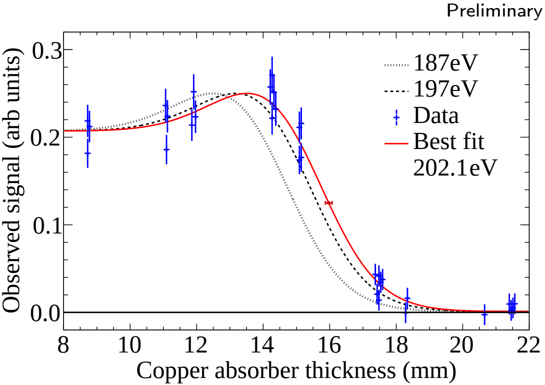

- Observe Bragg peak: Broadened by beam ΔE, range straggling
- Range is clearly longer than predicted by I-value of GAr
- Stats-only result: (202 ± 1) eV

Systematic uncertainties

Uncertainty	eV
Multiple Coulomb scattering model	2.1
Beam energy	1.5
Density×thickness of all materials	1.1
Scintillator response	1.0
Copper I-value	0.7
Alignment	0.4
All others, summed:	0.4
Composition of 6061 aluminum	
I-values of non-LAr materials	
Hadronic cross-sections	
Straggling model	
Fermi density effect model	
Total	3.2

- Systematically dominated
- Largest contribution from MCS
  - Uncertainty set by comparison of Geant4 EM "Opt0" to "Opt4" (EMZ)
- 2nd: Beam central energy (402.2 ± 0.2) MeV
  - The **proton** energy, from (402.7 ± 0.2) MeV H^-
  - Recently determined by accelerator experts from circumference and tuned RF frequency of the Booster, plus other cross checks
  - Beam energy spread is easier to measure and well-controlled
- 3rd: Material accounting
  - Biggest contribution from the density of 6061 aluminum: (2.69 ± 0.1) g/cc

Combination

- Review of historical data gives (197 ± 7) eV for LAr
- I measured (202 ± 4) at the Fermilab Linac *(paper in preparation)*
- Combining all information, I recommend (201 ± 3) eV (gray band)

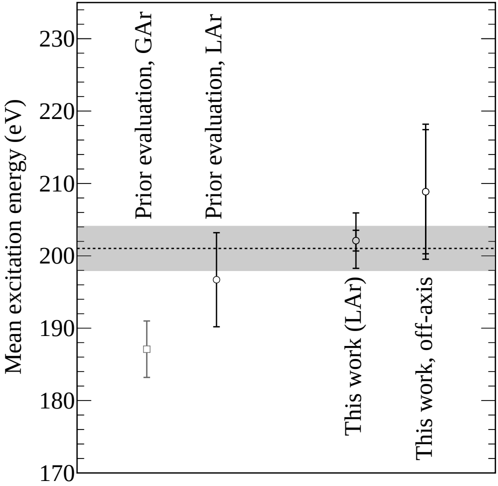

Implications for LAr experiments

- If you run MC for a LAr experiment, you should change the I-value to 201 eV
  - `G4Material::GetIonisation()->SetMeanExcitationEnergy(201*eV)`
- Effect on a long-baseline (or short-baseline) experiment:
  - Increase proton and muon ranges by $\sim 0.5\%$
  - Decrease muon dE/dx by $\sim 0.5\%$
  - $\Rightarrow$ reconstructed energies change by $\sim 0.5\%$
  - No near/far cancellation
  - Shifts $\Delta m^2_{32} \sim 0.5\%$
- With this recommendation, systematic uncertainty on Δm^2_{32} from LAr I-value is $\sim 0.2\%$
  - Using only published results, $\sim 0.5\%$ uncertainty on Δm^2_{32}

- DUNE currently says 0.3% sensitivity with large exposures
- Need to use better I-value, take I-value uncertainty into account

DUNE Neutrino 2024

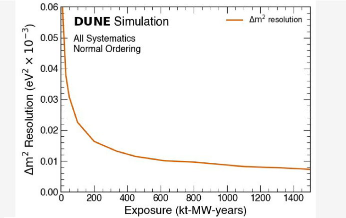

Conclusions

- Mean excitation energy of liquid argon is an important parameter for modern experiments
- The commonly-used 188 eV, from a 1984 evaluation of gaseous argon, is not good enough
- From (primarily) OSD, phase effect trends, plus a new 2024 range experiment, I recommend (201 ± 3) eV for LAr
- I-values of other experimental materials
  - Existing measurements sometimes good enough, sometimes calibration compensates
  - Sometimes not
  - Commonly based on very old data with various problems
    - No uncertainties
    - Unknown CL of uncertainties
    - Inadequate explanation of uncertainties
    - Only one measurement
    - Not peer reviewed
    - Etc.
  - Measurements relatively easy, any requests?

Backups

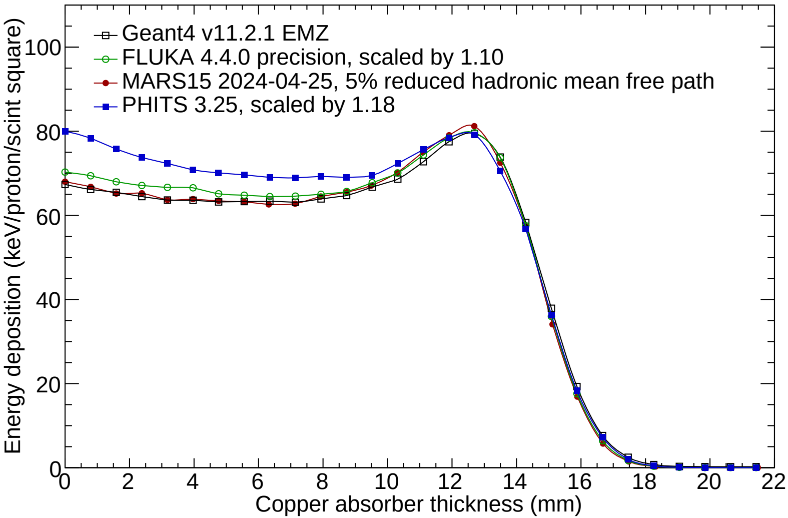
Geant4 v11.2.1 EMZ
FLUKA 4.4.0 precision, scaled by 1.10
MARS15 2024-04-25, 5% reduced hadronic mean free path
PHITS 3.25, scaled by 1.18
Energy deposition (keV/proton/scint square)
Copper absorber thickness (mm)
0
20
40
60
80
100
0
2
4
6
8
10
12
14
16
18
20
22